Supporting Information

Antioxidant Properties of Cerium Oxide Nanocrystals as a Function of Nanocrystal Diameter and Surface Coating

Seung Soo Lee,[†] Wensi Song,[‡] Minjung Cho,[†] Hema L. Puppala,[†] Phuc Nguyen, [†] Huiguang Zhu,[†] Laura Segatori,[‡] and Vicki L. Colvin[†,‡,]*

†Department of Chemistry, Rice University, Houston TX 77005 USA.

‡Department of Chemical and Biomolecular Engineering, Rice University, Houston TX 77005 USA.

*Corresponding author: colvin@rice.edu

Phase transfer of cerium oxide nanocrystal

The as-synthesized nanoceria was covered with oleylamine and stable in various non-polar solvents (*e.g.* chloroform, hexane, and toluene). When oleic acid was added to oleylamine covered nanoceria, the hydrophobic-hydrophobic interaction occurred and made nanoceria soluble in water because of the carboxyl groups on the outer surface of nanoceria. The addition of PAAOA and PMAO is similar to the oleic acid bilayer method, resulting in double layers. Both amphiphilic polymers have long hydrophobic chains (octylamine of PAAOA, and 1-octadecene of PMAO) forming a double layer with oleylamine on the surface of nanoceria. PEI has a large number of amine groups and hence, makes nanoceria soluble in water by ligand exchange method.

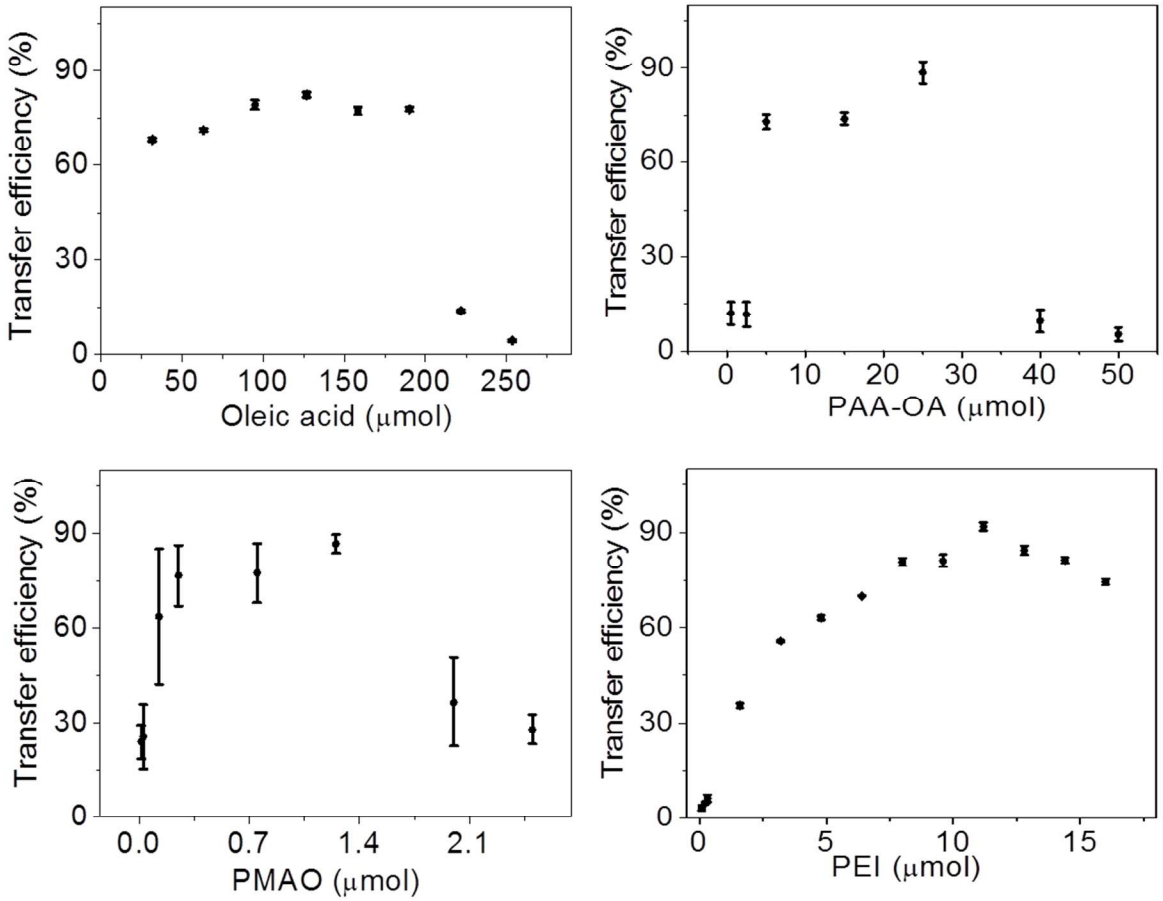

Figure S1. Phase transfer efficiency of water soluble nanoceria coated with 4 different phase transfer agents. Lower concentration of phase transfer agents (oleic acid, PAAOA, PMAO and PEI) caused poor surface coverage that led to highly aggregated cerium oxide precipitates, which were not dispersible in

water. Yet, higher concentration of phase transfer agents did not guarantee an increase in phase transfer efficiency because excess amount of surfactants formed micelles. These micelles lowered the solubility of water-soluble nanoceria.[1] In some case, the error bars are not larger than the symbol height.

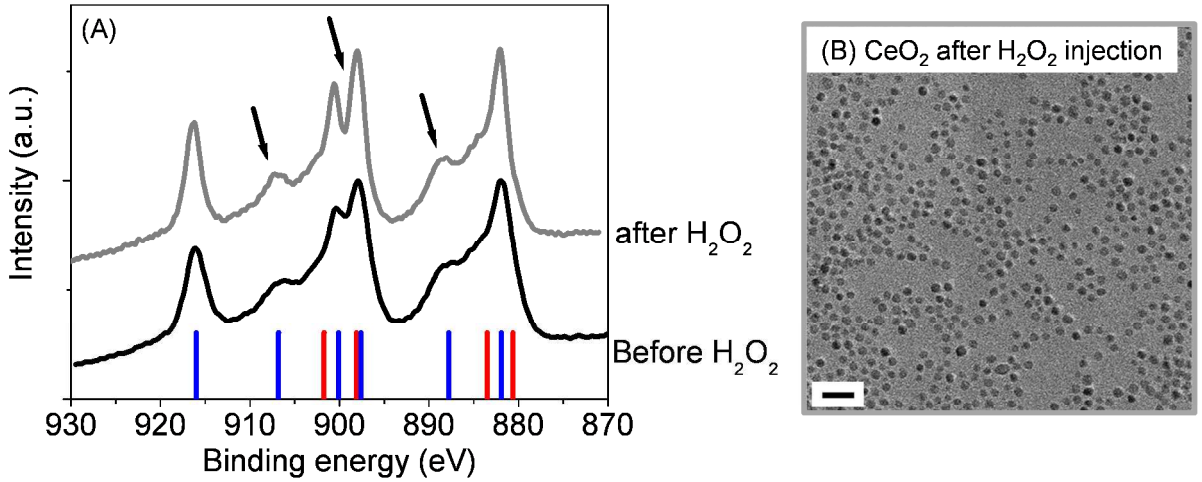

Figure S2. CeO_2 nanocrystals before and after peroxide injection. (A) XPS data of 3.8 nm CeO_2 before and after H_2O_2 injection. At the bottom of the chart, blue and red vertical lines stand for Ce(IV) and Ce(III), respectively. The arrow points reveal the clear difference between before and after H_2O_2 injection. Concentration of Cerium (III) and Cerium (IV) were calculated by the integration of the individual peaks from the fitted curve by MultiPak V7.0.1 (Table S1). (B) TEM image of cerium oxide nanocrystals after H_2O_2 injection. Scale bar is 20 nm.

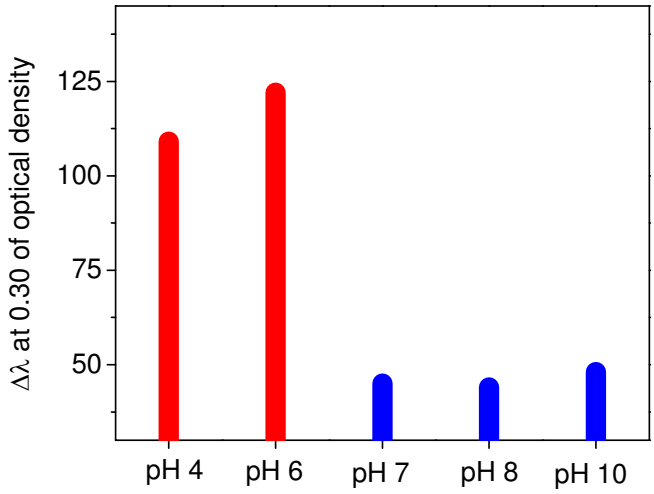

Figure S3. PH dependent antioxidant capacity of oleic acid coated cerium oxide suspension. Nanocrystalline ceria was more reactive with H_2O_2 in the less acidic condition than neutral and basic. However, oleic acid coated ceria nanocrystal (pH<6) lost the colloidal stability resulting in the precipitates after 1 day.

The calculation of the concentration of cerium oxide nanocrystals using the molecular weight of a cerium oxide nanocrystal

The concentration nanocrystalline cerium oxide was also calculated using the density of bulk cerium oxide and percentage of cerium (III) from XPS analysis. Briefly, to get the weight of one nanocrystal, the density of CeO_{2-x} was calculated based on the density of cerium oxide (CeO_2 :7.6 g/ml; Ce_2O_3 : 6.2 g/ml), and 44 % of cerium (III) obtained by XPS analysis; the calculated density of CeO_{2-x} was about 7.0 g/ml. Then the molecular weight of a 3.8 nm cerium oxide nanocrystal was obtained using the volume of one 3.8 nm nanocrystal analytical and the Avogadro's number. For example, the volume of one nanocrystal is 2.87×10^{-20} cm^3, which provides the weight of a nanocrystal of 2.0×10^{-19} g and the weight of one mole of nanocrystal of 121218.13 g/mol. Since the cerium concentration measured by ICP is 300 mg/L, the total concentration of 3.8 nm cerium oxide nanocrystal suspension is 3.03 μM (0.0091 μmol). This is very close to the number of nanocrystal concentration described in the experimental section: 2.78 μM of cerium oxide nanocrystal concentration.

The calculation of Ce(III) ions on the surface of one nanocrystal[2]

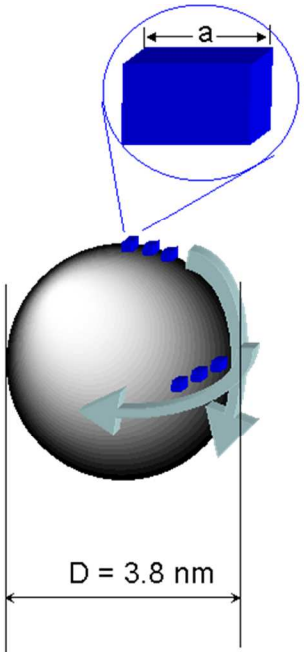

Figure S4. The calculation of the number of unit cells on the surface of 3.8 nm cerium oxide nanocrystal.

The number of Ce ions in one unit cell (Cubic fluorite) = 4 ions (8 at corners and 6 on the faces)

Let us consider that there is an outer shell of atoms surrounding the core of the nanoparticle. Thickness of this shell = $\frac{1}{2} \times 5.39 \times 10^{-10} = 2.69 \times 10^{-10}$ (m) (Thickness of the shell is assumed to be a half of the lattice constant.)

Volume of the core = $\frac{4}{3} \times 3.14 \times (1.9 \times 10^{-9} - 2.69 \times 10^{-10})^3 = 1.82 \times 10^{-26}\ \mathrm{m}^3$

Volume of the cluster = $\frac{4}{3} \times 3.14 \times (1.9 \times 10^{-9})^3 = 2.87 \times 10^{-26}\,\mathrm{m}^3$

Volume of the shell = $2.87 \times 10^{-26} - 1.82 \times 10^{-26} = 1.06 \times 10^{-26}\,\mathrm{m}^3$

Volume of single unit cell (a^3) = $(5.39 \times 10^{-10})^3 = 1.57 \times 10^{-28}\,\mathrm{m}^3$

The number of unit cells on the shell of nanoparticle = Volume of the shell / Volume of single unit cell = $\frac{1.06 \times 10^{-26}}{1.57 \times 10^{-28}} = 67.4$ ea

Since each unit cell has 4 Ce ions, the number of Ce ions on the surface (shell) of nanoparticle = $4 \times 67.4 = 269.5$ ea

Base on the XPS study, Ce(III) is 44 % of Ce ions on the surface. Therefore, the number of Ce(III) is $269.5 \times 0.44 = 118.6 \approx 119$.

Concentration of cerium oxide nanoparticles = 2.78 μM

Volume of CeO_2 nanocrystal suspension = 3 ml

The number of Ce(III) in nanoceria solution =

N_A (particles/mol) $\times 8.34 \times 10^{-9}$ (mol) $\times 119$ (Ce(III)/particle) $= 9.9246 \times 10^{-7}\, N_A$ of Ce(III)

(N_A is avogadro's number = 6.02×10^{23} particles/mol)

Therefore, about 0.99246 μmol of Ce(III) is in the nanoceria solution.

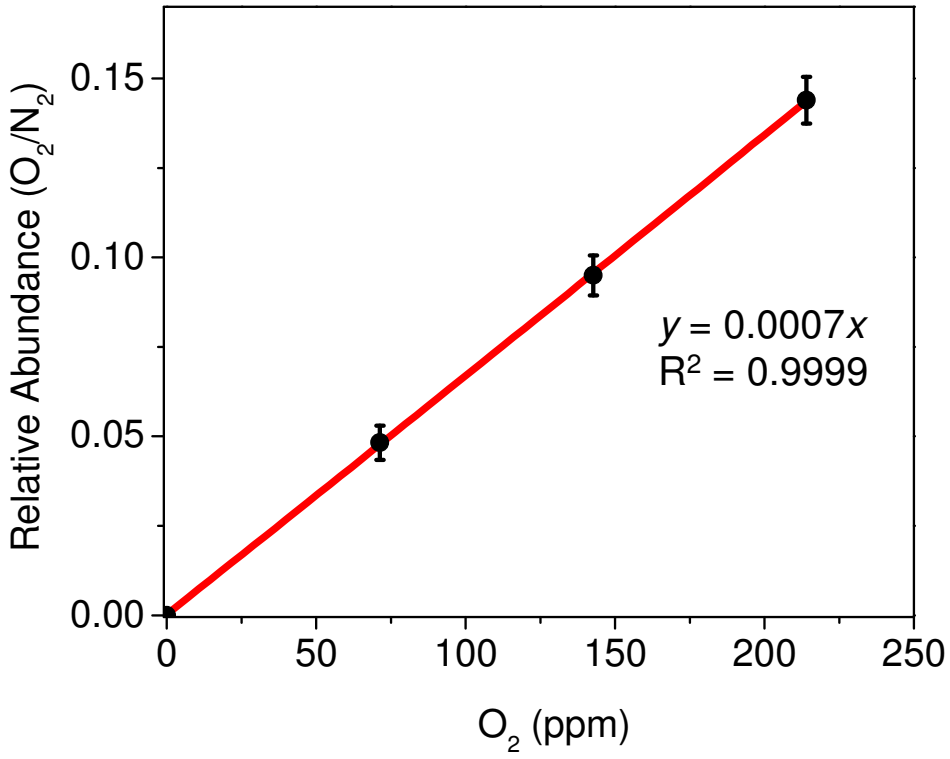

Figure S5. The calibration curve of O_2 in GC-MS analysis. O_2 concentration was measured using relative abundance between O_2 and N_2. For details, 10 ml crimped vials were sealed tightly and purged with N_2 for 5 min. Then, 500, 1000, and 1500 µl of O_2 were injected into N_2 purged vials and 10 µl of the sample was injected into GC-MS using Pressure-Lok gas syringe (VICI Precision Analytical Syringe, Vacuum leak rate was less than 2.8×10^{-3} µl/hr.). These measurements were repeated in triplicates. Concentration (ppm) was calculated by considering the purged vials to be at 1atm, and then getting mass of the oxygen.

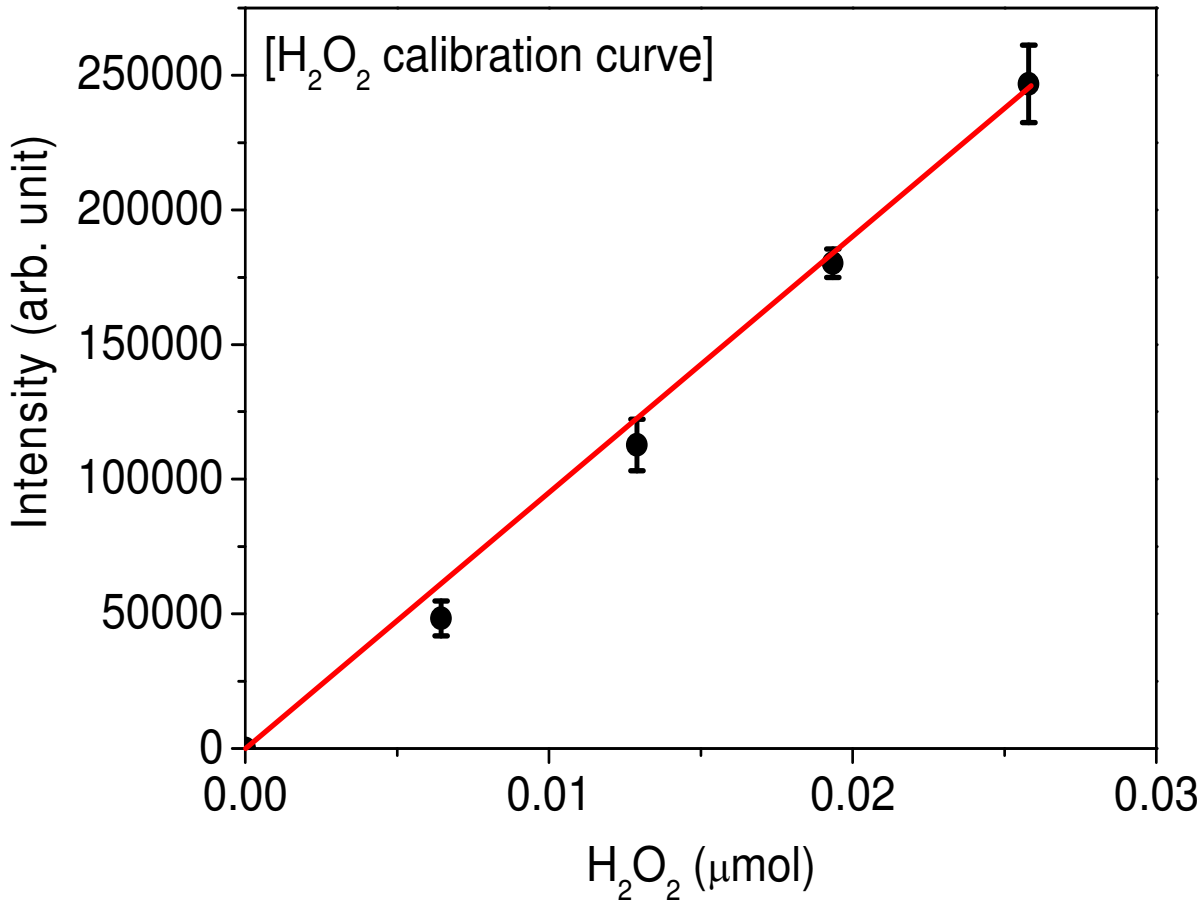

Figure S6. The H_2O_2 calibration curve for the luminol test. The calibration curve was obtained by measuring the chemiluminescence of luminol as a function of the increasing concentration of the injected H_2O_2 (from 0 to 0.03 μmol). The equation of the curve was $y = 9.0 \times 10^6 x$ with 0.994 of R^2. (y = the intensity of luminescence, x = mol of H_2O_2)

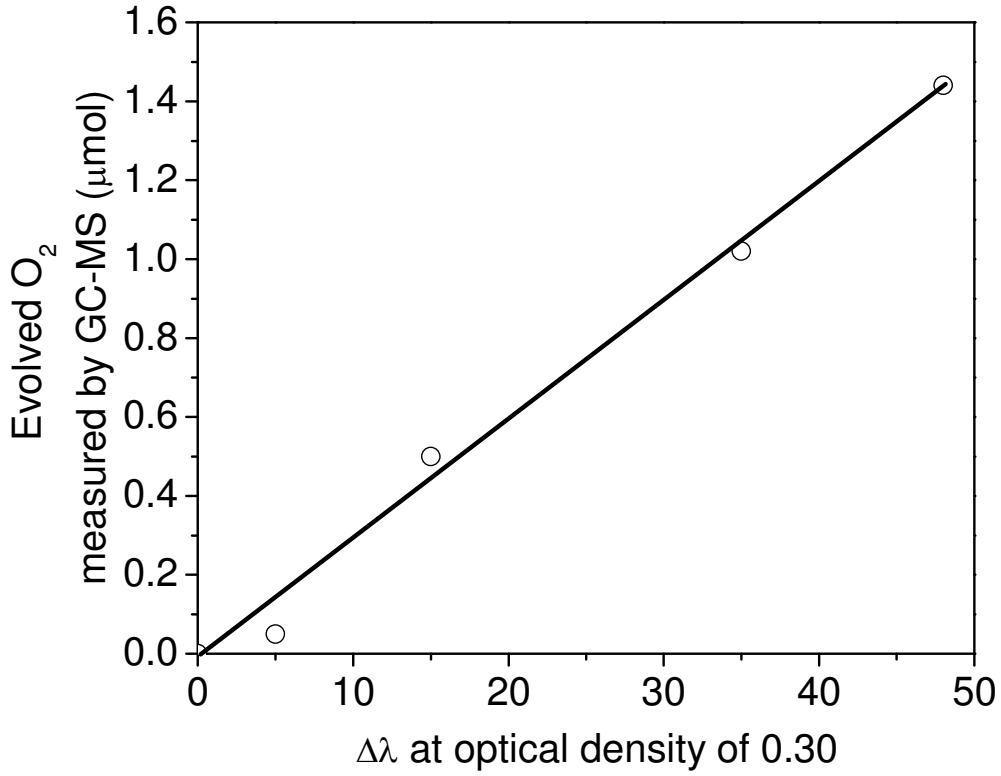

Figure S7. Decomposed H_2O_2 calculation using the red shift UV-Vis band and GC-MS data. Various molar concentrations of H_2O_2 (0, 0.1, 1, 5, 10 μmol) were injected into ceria nanocrystal suspensions (1 μmol of cerium (III) concentrations on the nanocrystals in the suspension). The decomposed H_2O_2 based on the measurement using GC-MS (Figure 4) was plotted as a function of the wavelength difference between the red shift UV-Vis band and the control at optical density of 0.30. The equation of the trend line was $y = 0.0298x$ (y is the evolved O_2 (μmol) and x is the Δλ at optical density of 0.30) and $R^2 = 0.9915$. Using this equation and the disproportionation of H_2O_2 ($2H_2O_2 \rightarrow 2H_2O + O_2$), the total moles of the decomposed H_2O_2 were calculated in the multiple injections of H_2O_2 as shown in Figure 8. For example, oleic acid coated CeO_2 suspension under the multiple H_2O_2 injections showed 21.6 μmol of H_2O_2 decomposition for 18 cycles. (1 μmol of H_2O_2 was injected in every cycle.)

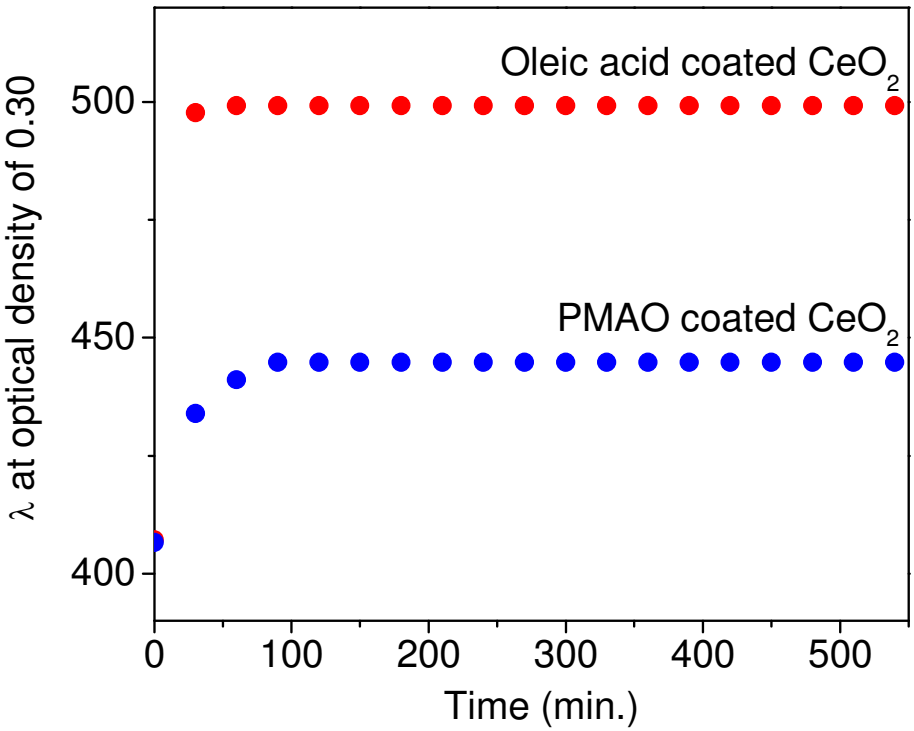

Figure S8. The magnitude of the red shift UV-Vis band of oleic acid and PMAO coated ceria nanocrystal suspension after H_2O_2 injection. 1 mmol of H_2O_2 was injected in 2.78 μM of ceria nanocrystal suspension and the wavelength at optical density of 0.30 was measured as a function of time (min). Oleic acid coated CeO_2 was saturated quickly with the higher red-shifted UV-Vis band as compared to PMAO coated one.

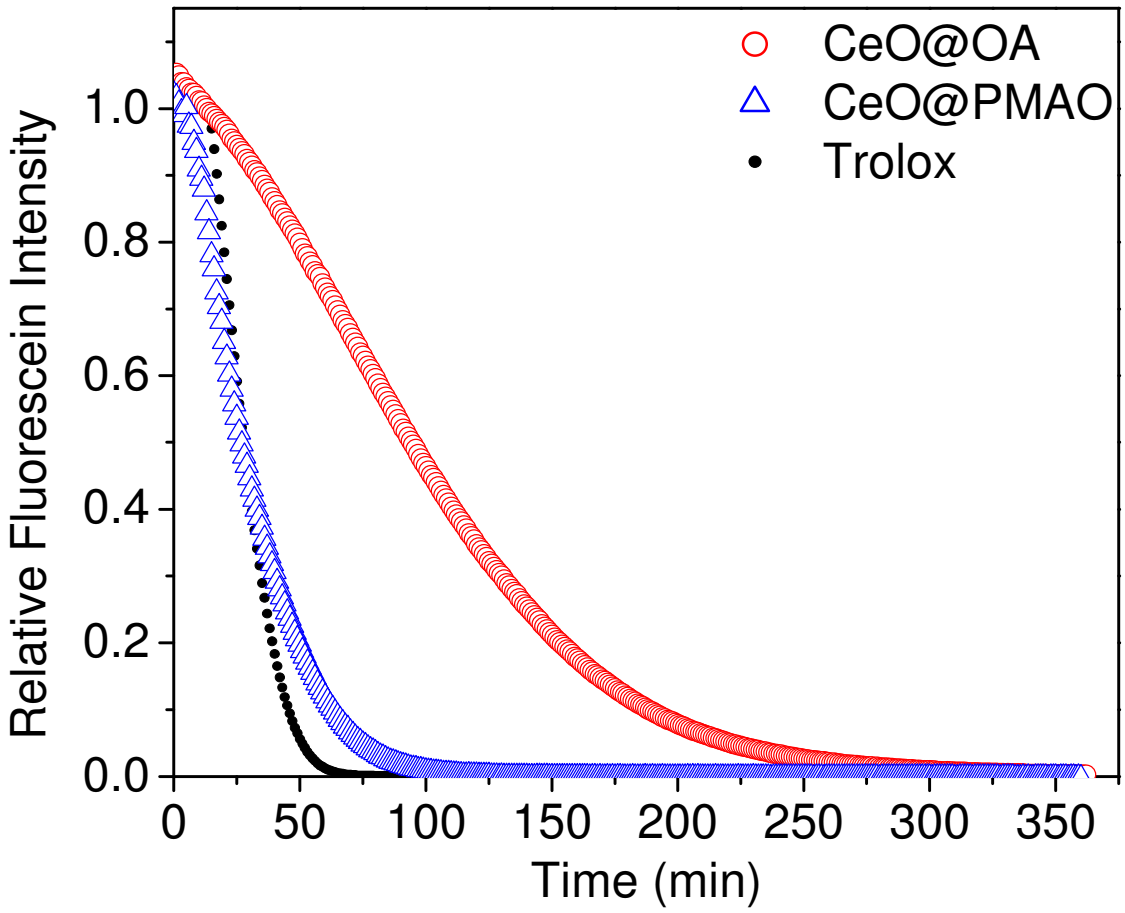

Figure S9. Oxygen-radical absorbance capacity (ORAC) assay of oleic acid coated – (red), PMAO coated – (blue) nanoceria and Trolox (black). The concentration of cerium oxide nanocrystals (the number of nanocrystals in the suspension; see the experimental section) and Trolox ($C_{14}H_{18}O_4$; mass of trolox was divided by the molar mass of 250.29 g/mol) was 0.8 μM. Fluorescence was measured every minute for 6 hrs. In order to characterize the percentage of the antioxidant capacity of given substances, the area under curve (AUC) was calculated from each graph and divided by the AUC of the blank sample (see the experimental section).

Cell viability test using water soluble cerium oxide nanocrystals

Cell Culture: Human dermal fibroblasts (HDF, Cambrex) were purchased from Cambrex and cultured in Dulbecco's Modified Eagle's Medium (DMEM, ATCC, Manassas, VA), supplemented with 2 mM L-glutamine, 1% penicillin, 1% streptomycin, and 10% fetal bovine serum (FBS). Cells were detached from culture with trypsin and re-suspended in media for passaging to wells. Cells were used at passages from 3 to 6 for experiments.

MTS cell viability assay: The standardized colorimetric assay, MTS (CellTiter 96, Promega), was used to evaluate mitochondrial activity. HDF cells were grown to 80 % confluency in 96-well culture plates and introduced to 3.8 nm oleic acid coated nanoceria (from 0 to 3.1 μM of nanocrystal concentrations. The treated cells were incubated for 24 at 37 °C under 5% CO_2. Then, the supernatant containing the nanocrystals was removed from the wells and replaced with 100 μL of fresh DMEM that is phenol-red free (Gibco/Invitrogen); 20 μL MTS stock solution was added to each well. The MTS assay is reduced by enzymes in live cells, producing a purple formazon dye. After incubating at 37 °C for 1 h, the absorbance at 490 nm of the dye produced was measured using a plate reader (TECAN Infinite M200). Each experiment was repeated four times to obtain the average value.

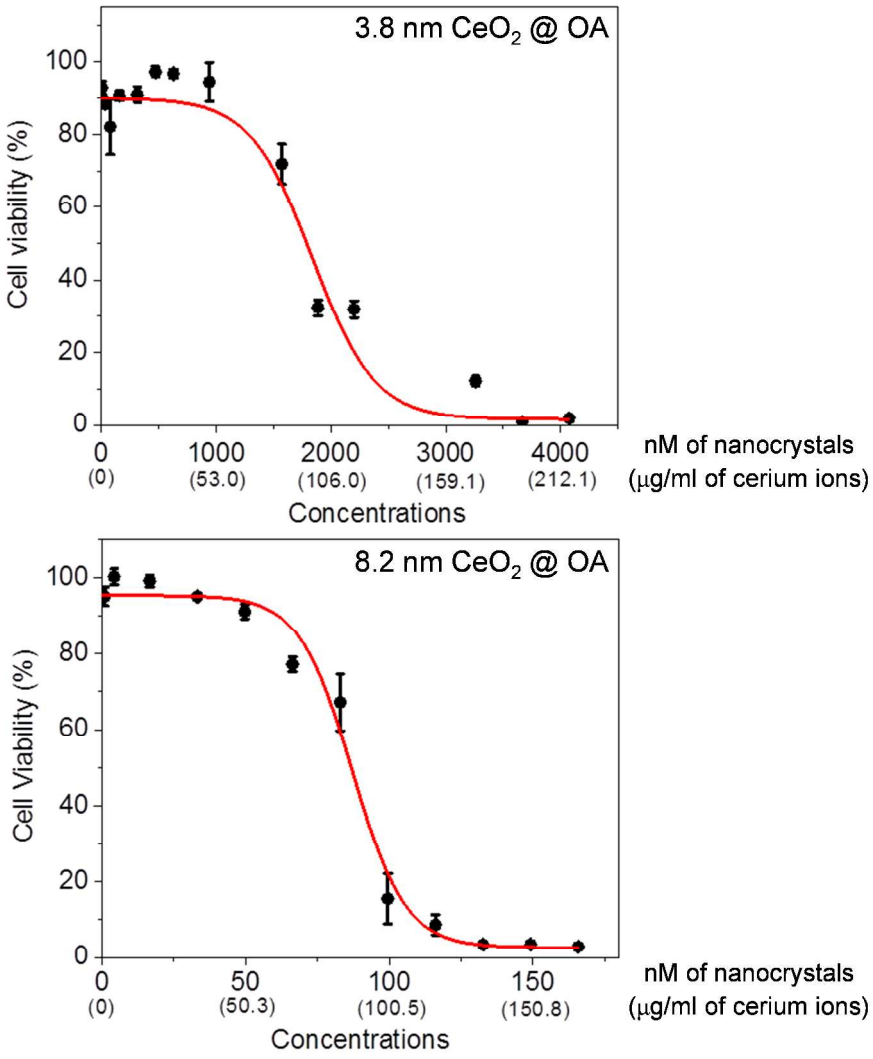

Figure S10. Cell viability of Human Dermal Fibroblast (HDF) cell line in the presence of 3.8 and 8.2 nm coated cerium oxide nanocrystals coated with oleic acid. In the MTS analysis, HDF cells exhibited a decrease in viability as ceria nanocrystal concentration increased. A acute cell viability assay revealed that a LD_{50} value for 3.8 nm cerium oxide nanocrystals coated with oleic acid was 1.8 μM (94.9 ppm), and for 8.2 nm cerium oxides, 87.2 nM (87.7 ppm). The ORAC assay using trolox and 3.8 nm cerium oxides in Figure 7 was treated under the concentration of 1000 nM (0.15, 0.5, 0.8, and 1 μM).

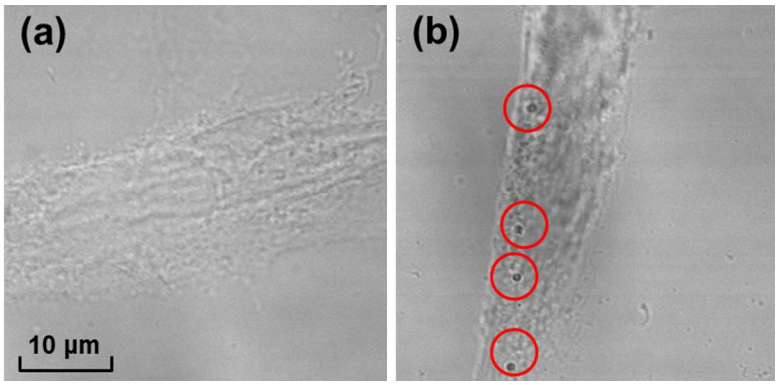

Figure S11. Bright field images of human dermal fibroblasts treated with cerium oxide nanocrystals. Fibroblasts were seeded on glass coverslips, cultured in the presence of cerium oxide nanocrystals for 24 h at 37 °C, and fixed with 4% paraformaldehyde for 30 min. Bright field images were obtained using an Olympus IX81 confocal microscope. (a) Cells cultured without cerium oxide nanocrystals. (b) Cells cultured in medium supplemented with cerium oxide nanocrystals. The nanocrystals are highlighted with red circles.

Measurement of the nanocrystal concentration in cells

The intracellular concentration of the nanocrystals was analyzed using Inductively coupled plasma mass spectrometry (ICP-MS; Perkin Elmer ELAN9000) as previously described by Ma, X. *et al.*[3] 10^5 fibroblasts were plated in each well of 6-well plates and incubated overnight to allow cell attachment. Cells were incubated with cerium oxide nanocrystals for 24 h. Cells were then washed with PBS and water, and incubated with acidic solution (50 mM glycine, 100 mM sodium chloride, 2 mg/ml polyvinylpyrrolidone (MW: 40K), pH 3) to separate membrane-binding nanocrystals by acid stripping.[4] After removing membrane proteins, cells were collected and digested with 1% HNO_3. To estimate the amount of cerium oxide nanocrystals internalized by the cells, ICP-MS was used. The concentration of cerium atoms in each well was measured and the number of cerium oxide nanocrystals was calculated based on the number of atoms in each particle as previously described.[5] Table S2 shows that both nanocrystals (3.8 nm and 8.2 nm cerium oxide nanocrystals) were found from the intracellular organelles after removing the cell membranes; the number of 3.8 nm cerium oxides was 1.71×10^6 nanocrystals and that of 8.2 nm cerium oxides was 2.15×10^4 nanocrystals in the cells.

Reuse and recycling of nanocrystalline ceria in reactions with hydrogen peroxide

Ceria nanocrystals with the highest quenching capacity for peroxide in a single injection did not necessarily fare well upon repeated injections. PEI coated nanoceria precipitated after exposure to 10 μmol of H_2O_2. However, ceria nanocrystals coated with amphiphiles (PAAOA, oleic acid, and PMAO) showed repeated H_2O_2 reactivity and cerium (III) recovery without precipitation (Figure S12 and S13). Overall oleic acid ceria nanocrystals were the most stable materials in redox cycling experiments. Figure S12 shows the reactivity of PAAOA, oleic acid, and PMAO coated nanoceria (d= 3.8 nm) after the repeated injection of H_2O_2 as a function of time. Both the thinnest and thickest bilayer surface coatings (oleic acid and PMAO) remained stable in solution even after treatment with more than 70 μmol of H_2O_2 during multiple injections over 3 months; PAAOA coated nanoceria yielded precipitates after exposure to 30 μmol H_2O_2. In case of larger diameter of nanoceria, 5.4 and 8.2 nm cerium oxides coated with oleic acid were stable for about 45 and 70 days up to reactions with 40 μmol of H_2O_2, respectively. However PEI coated nanoceria precipitated quickly. We speculate that the weak interaction between cerium oxide and the amine group functionalized polymer (PEI) makes them generally less stable as peroxides are reacting with the surfaces. Furthermore, it is possible that the H_2O_2 molecules have not only reacted with cerium (III) on the core particle but may also attack the coating itself resulting in nanocrystal aggregates.[6]

If too much H_2O_2 is added to the solution (*e.g.* more than a fivefold excess) then samples have less ability to undergo multiple reactions. When the molar ratio between H_2O_2 and cerium (III) was 1:1 and 0.1:1, nanoscale ceria exhibited long-term redox cycling as described above (Figure S14). When H_2O_2 molecules are not in excess compared to the cerium (III), peroxide will preferentially react with cerium (III). In contrast, under conditions of excess H_2O_2 (*e.g.* more than 10X cerium (III)) the redox cycling is less frequently observed and instead nanocrystals aggregated and exhibit reduced reactivity towards hydrogen peroxide.[7-9]

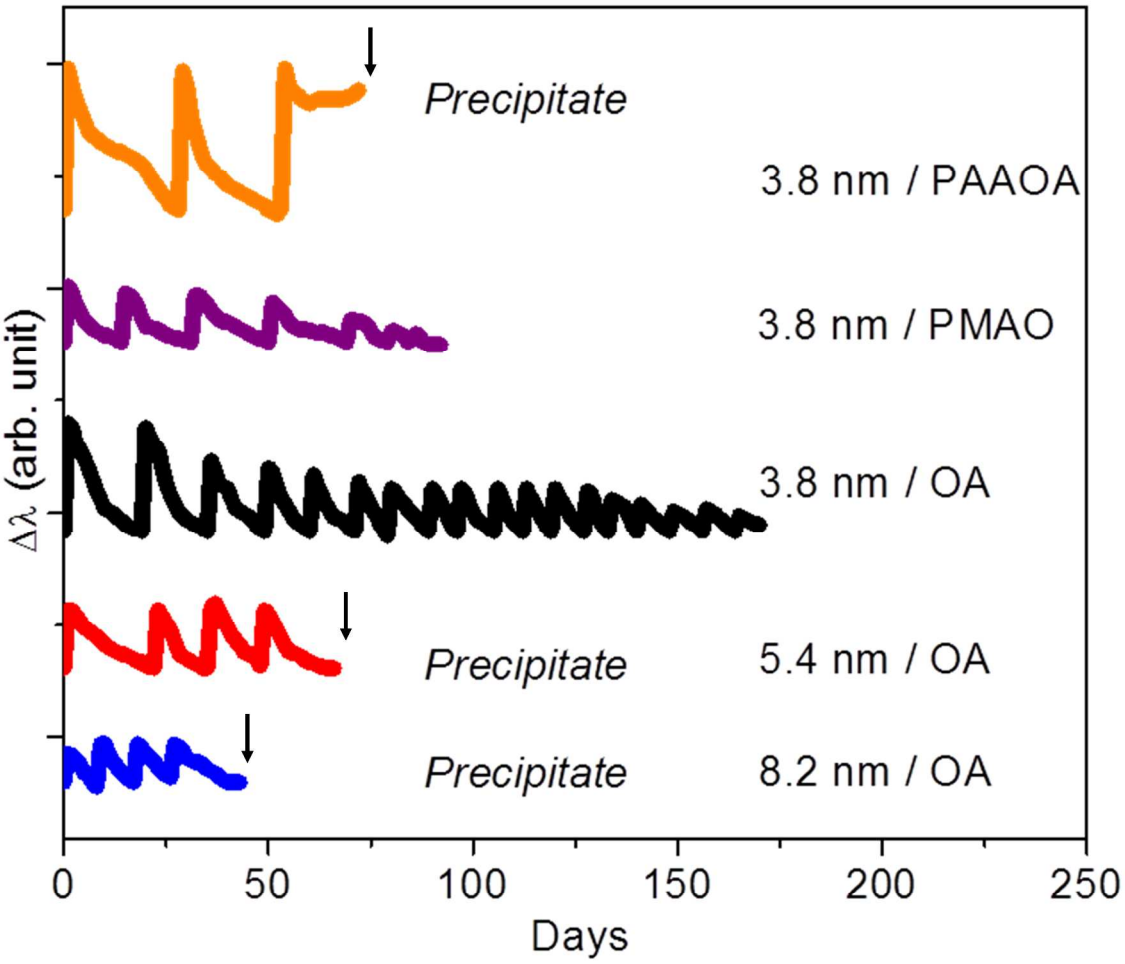

Figure S12. Antioxidant property of water-soluble nanoceria coated with bilayer surface structures. PAAOA, oleic acid (OA), and PMAO coated nanoceria in diameter of 3.8, 5.4, and 8.2 nm were utilized. All cerium oxide nanocrystal concentrations were 2.78 μM (Cerium (III) concentration on the surface of nanocrystal: 1 μmol) and 10 μmol of H_2O_2 was injected in every cycle. The wavelength (λ) of the red-shifted UV-Vis band was monitored at optical density of 0.30 abs as a function of time. UV band was recovered as time goes on and the additional injections of H_2O_2 gave rise to the red-shift, again. However, the multiple injections of H_2O_2 led to the reduction in quenching property (the extent of Δλ) of nanoceria suspension. 3.8 nm PMAO and oleic acid (OA) coated cerium oxide did not show any visible precipitate but the H_2O_2 quenching property decreased by multiple injection of H_2O_2. PAAOA coated cerium oxide was precipitated after 3rd injection of H_2O_2 and 5.4 and 8.2 nm OA coated CeO_2 was precipitated after 4th addition of H_2O_2. PEI coated CeO_2 was never recovered from the 1st injection of H_2O_2 and lost its colloidal stability.

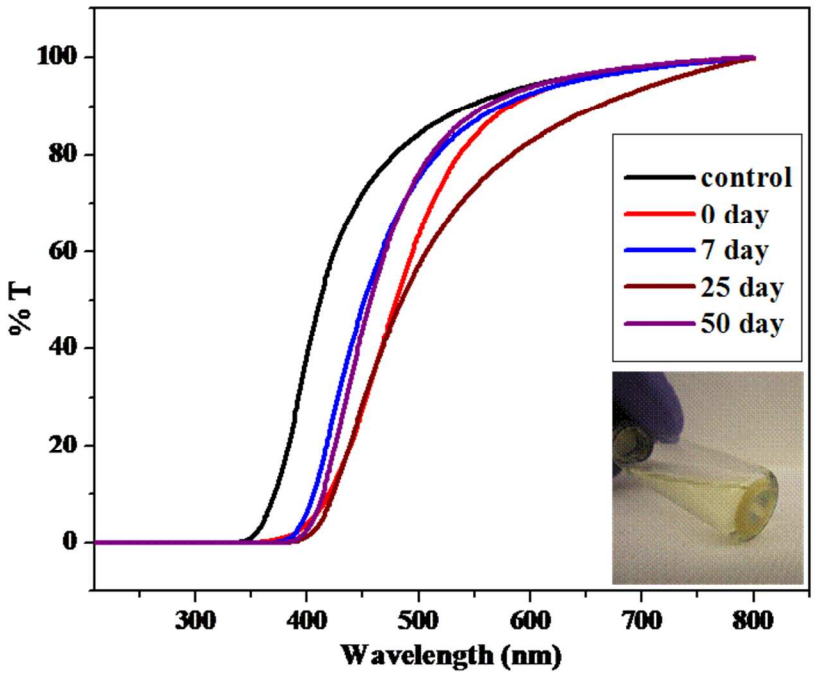

Figure S13. Loss of colloidal stability of PEI coated 3.8 nm nanoceria after H_2O_2 injection. UV-Vis band was monitored over time. The red-shift UV-Vis band was not recovered to the control. The inset photograph showed precipitates at the bottom of the sample containing PEI coated nanoceria in 50 days after the injection of H_2O_2.

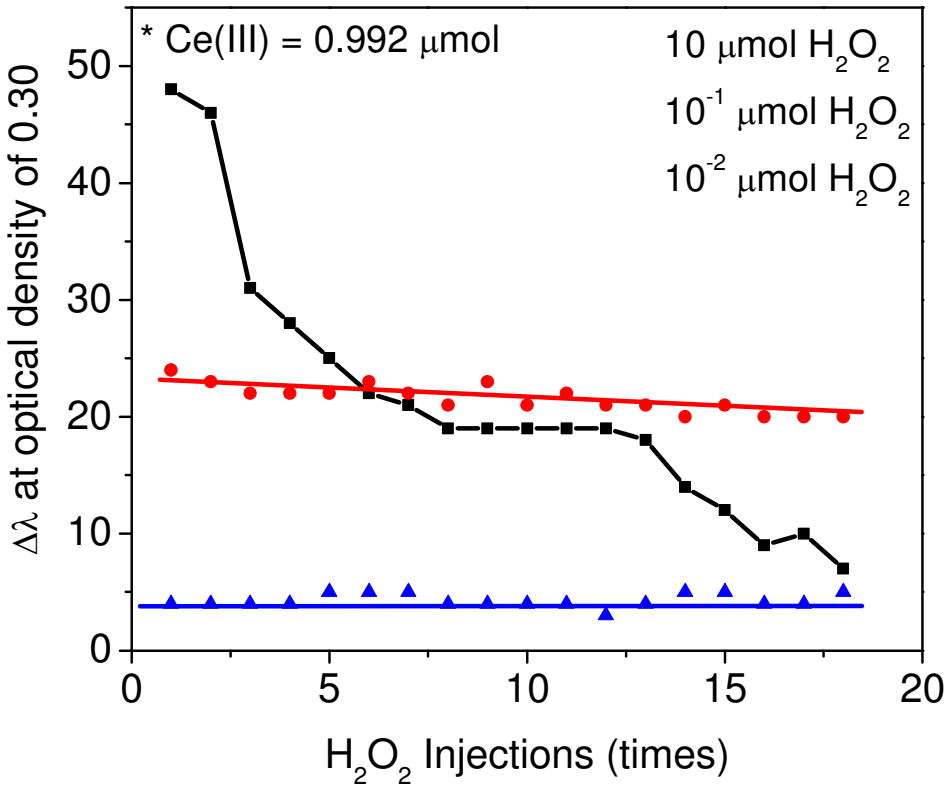

Figure S14. Antioxidant capacity of ceria nanocrystal suspension (2.78 μM of nanocrystal concentration: 1 μmol of cerium (III) concentration) depending on different amount of H_2O_2 injections for 18 cycles. The excess H_2O_2 (black line) led to the decrease in the magnitude of the red shift of UV-Vis band from the control ($\Delta\lambda$) but the same (red line) and lower (blue line) amount of H_2O_2 injection than cerium (III) showed the consistency of the antioxidant capacity without losing the colloidal stability.

Table S1. XPS analysis of individual peaks. Cerium (III) concentration was calculated by (V_1 + V_3+ V_6 + V_8). [5, 10-14] The ten individual peaks (from V_1 to V_{10}) were integrated in the cerium 3d region from 880 to 916 eV of the binding energy as shown in Figure S2.

	Size (nm)	V_1	V_2	V_3	V_4	V_5	V_6	V_7	V_8	V_9	V_{10}	%Ce(III)
Before H_2O_2 Injection	3.8	4.05 (880.64)	8.12 (881.93)	17.16 (883.54)	14.07 (887.84)	9.86 (897.66)	8.87 (898.39)	5.52 (900.18)	12.66 (901.77)	9.89 (906.62)	9.81 (916.01)	42.74
After H_2O_2 Injection	3.8	2.08 (881.04)	15.29 (882.42)	4.26 (884.32)	21.77 (887.31)	9.98 (897.58)	0.54 (898.14)	13.11 (899.77)	13.47 (902.23)	10.72 (906.80)	8.79 (916.56)	20.35

Table S2. Number of cerium oxide nanocrystals in cells. Cells were plated at a concentration of 1.0×10^5 cells/well. The average number and the standard deviation of cerium oxide nanocrystals were from triplicate measurements.

	Conc. of Ce (ppm)		The number of the nanocrystals per well		The number of the nanocrystals per cell	
	Average	Standard deviation	Average	Standard deviation	Average	Standard deviation
CeO_2 (3.8 nm)	0.1007	0.0041	1.71×10^{11}	6.42×10^{9}	1.71×10^{6}	6.42×10^{4}
CeO_2 (8.2 nm)	0.0240	0.0014	2.15×10^{9}	2.06×10^{8}	2.15×10^{4}	2.06×10^{3}

REFERENCES

1. Murakami, K.; Chan, S. Y.; Routtenberg, A., Protein-Kinase-C Activation by Cis-Fatty Acid in the Absence of Ca^{2+} and Phospholipids. *J. Biol. Chem.* **1986,** *261*, 5424-5429.
2. Binns, C., *Introduction to nanoscience and nanotechnology*. Wiley: Hoboken, N.J., 2010.
3. Ma, X.; Wu, Y.; Jin, S.; Tian, Y.; Zhang, X.; Zhao, Y.; Yu, L.; Liang, X. J., Gold Nanoparticles Induce Autophagosome Accumulation Through Size-Dependent Nanoparticle Uptake and Lysosome Impairment. *ACS Nano* **2011,** *5*, 8629-8639.
4. Hassan, A. A.*, et al.*, Serine-Derivatized Gadonanotubes as Magnetic Nanoprobes for Intracellular Labeling. *Contrast Media Mol. Imaging* **2010,** *5*, 34-38.
5. Lee, S. S.; Zhu, H. G.; Contreras, E. Q.; Prakash, A.; Puppala, H. L.; Colvin, V. L., High Temperature Decomposition of Cerium Precursors To Form Ceria Nanocrystal Libraries for Biological Applications. *Chem. Mater.* **2012,** *24*, 424-432.
6. Breccia, J. D.; Andersson, M. M.; Hatti-Kaul, R., The Role of Poly(Ethyleneimine) in Stabilization against Metal-Catalyzed Oxidation of Proteins: A Case Study with Lactate Dehydrogenase. *BBA-Gen. Subjects* **2002,** *1570*, 165-173.
7. Noureddini, H.; Kanabur, M., Liquid-Phase Catalytic Oxidation of Unsaturated Fatty Acids. *J. Am. Oil Chem. Soc.* **1999,** *76*, 305-312.
8. Swern, D.; Billen, G. N.; Findley, T. W.; Scanlan, J. T., Hydroxylation of Monounsaturated Fatty Materials with Hydrogen Peroxide. *J. Am. Chem. Soc.* **1945,** *67*, 1786-1789.
9. Turnwald, S. E.; Lorier, M. A.; Wright, L. J.; Mucalo, M. R., Oleic Acid Oxidation Using Hydrogen Peroxide in Conjunction with Transition Metal Catalysis. *J. Mater. Sci. Lett.* **1998,** *17*, 1305-1307.
10. Deshpande, S.; Patil, S.; Kuchibhatla, S. V. N. T.; Seal, S., Size Dependency Variation in Lattice Parameter and Valency States in Nanocrystalline Cerium Oxide. *Appl. Phys. Lett.* **2005,** *87*, 133113.

11. Kar, S.; Patel, C.; Santra, S., Direct Room Temperature Synthesis of Valence State Engineered Ultra-Small Ceria Nanoparticles: Investigation on the Role of Ethylenediamine as a Capping Agent. *J. Phys. Chem. C* **2009,** *113*, 4862-4867.
12. Korsvik, C.; Patil, S.; Seal, S.; Self, W. T., Superoxide Dismutase Mimetic Properties Exhibited by Vacancy Engineered Ceria Nanoparticles. *Chem. Commun.* **2007**, 1056-1058.
13. Qiu, L. M.; Liu, F.; Zhao, L. Z.; Ma, Y.; Yao, J. N., Comparative XPS Study of Surface Reduction for Nanocrystalline and Microcrystalline Ceria Powder. *Appl. Surf. Sci.* **2006,** *252*, 4931-4935.
14. Tsunekawa, S.; Fukuda, T.; Kasuya, A., X-ray Photoelectron Spectroscopy of Monodisperse CeO_{2-x} Nanoparticles. *Surf. Sci.* **2000,** *457*, L437-L440.